This is the Pre-Published Version.

Wang, J., Liu, Z. Improving GNSS PPP accuracy through WVR PWV augmentation. J Geod 93, 1685–1705 (2019)

Improving GPS PPP Accuracy through WVR PWV Augmentation

Jungang Wang[a,b], Zhizhao Liu[a]*

a Department of Land Surveying & Geo-Informatics, Hong Kong Polytechnic University, Hung Hum, Kowloon, Hong Kong

b College of Surveying and Geo-Informatics, Tongji University, Shanghai, China

* Correspondence to: Z. Liu, Department of Land Surveying & Geo-Informatics, Hong Kong Polytechnic University, Hung Hum, Kowloon, Hong Kong. E-mail: lszzliu@polyu.edu.hk

Main point #1:
The PWV bias between GPS, WVR, ECMWF and radiosonde are compared and discussed using five months data at Shanghai, China.

Main point #2:
Difference PPP strategies to deal with ZTD, including estimating as unknown parameter, fixing with WVR data, meteorological data and GPT2 model are carried out in both static and kinematic mode.

Main point #3:
The influence of WVR in ZTD-fixed static PPP is investigated, and the benefits, including a better accuracy and the acceleration of convergence are demonstrated. In kinematic PPP mode the ZTD-fixed strategy using WVR data also shows a better accuracy. The accuracy of ZTD-fixed PPP using meteorological data and GPT2 is also investigated.

Abstract: This paper compares Precipitable Water Vapor (PWV) from GPS, Water Vapor Radiometer (WVR),

ECMWF and radiosonde in Shanghai, a mid-latitude costal city with high water vapor (with a mean value of 40 mm). Then a WVR assisted Precise Point Positioning (PPP) campaign is conducted, where ZTD is fixed using calibrated WVR observations and meteorological data. Also, another three PPP campaigns, where ZTD is estimated, fixed using meteorological data and GPT2 model are also carried out for comparison. All these four PPP campaigns are conducted in both static and kinematic modes, and for static mode, different cut-off elevation circumstances are applied. The PWV comparisons and PPP campaigns are based on about five months data, from June to October 2014. A big discrepancy as large as 2.4 mm bias between GPS PWV and WVR PWV is found and the corresponding RMS is about 3.2 mm. The discrepancy is treated as systematic bias and calibrated using a linear equation, with an RMS of 2 mm after calibration. Then the calibrated PWV from WVR are fixed in PPP solution. The results show that for static PPP in low cut-off elevation circumstances, WVR assisted PPP (with MAE of 1.7 cm and repeatability of 1.1 cm in up direction) has better accuracy than normal PPP solution (ZTD is estimated as unknown parameter), with an MAE of 1.8~2.0 cm and repeatability of 1.3 cm in up direction. In horizontal direction the accuracy of WVR assisted PPP is comparable with that of normal PPP solution, with an MAE of 0.8~1 cm, repeatability of 0.5 cm in North/East direction. For high cut-off elevation circumstance, WVR assisted PPP remains the same accuracy as low cut-off elevation circumstances, which is much better than that of normal PPP with a repeatability of 5 cm in up direction when the cut-off elevation is 30 degree. In addition, when ZTD is fixed using meteorological data or GPT2 model, due to the ZTD error the PPP accuracy is about 20 cm in low cut-off elevation circumstances and about 13 cm in high cut-off elevation circumstances. For kinematic PPP, calibrated WVR data also helps to achieve a better accuracy. In addition, WVR assisted PPP has a faster convergence time (with an mean value of 0.7 hours and median value of 0.5 hours) than that of normal PPP solution (more than 1 hour).

Key Words: Water Vapor Measurement; Water Vapor Radiometer; GPS Meteorology; GPS Precise Point

1 Introduction

As a highly variable constituent and the most important greenhouse of the atmosphere, water vapor has an important role in many physical processes and causes significant range delay to radio-based earth observation system such as Global Positioning System (GPS), Interferometric synthetic aperture radar (InSAR). Investigating the spatial distribution of water vapor is essentially important in GPS, InSAR and other observation systems. There are several techniques to monitor water vapor, including radiosonde (Miloshevich et al., 2006, 2009), Numerical Weather Model (NWM), water vapor radiometer (WVR) (Beckman, 1985). GPS has been used to the sounding of atmospheric water vapor since 1990s (Bevis et al, 1992; Duan et al., 1996; Rocken et al., 1997; Tregoning et al., 1998; Fang et al., 1998), and many researches have been conducted in the last decades (Liou et al., 2001; Gendt et al., 2004; Wang et al., 2005, 2007; Liu et al., 2013; Li et al., 2015).

Different from other water vapor retrieval techniques, water vapor radiometer can provide water vapor measurements of both high accuracy and high temporal resolution. Radiosonde usually has a temporal resolution of 12 hours. GPS usually can have water vapor sounding every one or two hours. However WVR can output water vapor measurements every 15 minutes. The WVR observation accuracy of 1~2 mm has been demonstrated. *Emardson et al.* (1998) reported the PWV difference between GPS and WVR are about 1~2 mm. *Rocken et al.* (2005) reported a bias of 1.2 mm and RMS of 2.8 mm between GPS PWV and WVR PWV. *Gunnar et al.* (2012) investigated the accuracy of WVR, GPS and VLBI in heavy rain days during CONT11. *Liou et al.* (2001) investigated the PWV difference in the tropical region with higher and more inhomogeneous water vapor burden, and demonstrated 2.2 mm difference between GPS and WVR. *Braun et al.* (2003) investigated the line-of-sight measurements of integrated water vapor from GPS and WVR with a RMS of 1.3 mm demonstrated. *Michal et al.* (2012) compared the GPS derived slant wet delay and direct measurements of WVR and reported that a simple mapping of zenith total delay into slant wet delay achieved the best accuracy than adding horizontal gradients or post-fit residuals.

Though the WVR water vapor data have been extensively studied and evaluated, the utilization of WVR observations in aiding GPS high precision positioning however has seldom been reported. *Ware et al.* (1993) reported a vertical precision of 2.6 mm on a 50 km baseline using WVR pointing toward GPS satellites to correct azimuthal PWV. *Liu et al.* (2013) evaluated different WVR regression accuracies of GPS, radiosonde, AERONET sunphotometer using GPS PPP and reported an accuracy of 3.8 mm with GPS regression algorithm, but the emphasis of that research was on the evaluation of different regression algorithms.

In this work, PWV data from one GPS and WVR co-located station at Tongji University, Shanghai, China (31°N, 121°E) is first compared. The water vapor data from a nearby radiosonde station and the ECMWF (European Centre for Medium-Range Weather Forecasts) are also used in the PWV comparison. To evaluate the impact of water vapor on PPP solutions, static and kinematic PPP tests are conducted by ingesting water vapor data, which are obtained from GPS ZTD estimated, and fixed using WVR data. Another two PPP solutions with ZTD fixed using GPT2 model and meteorological data are also conducted for comparison. In Section 2, the WVR and GPS data source and data processing method are described. The comparison of different sets of PWV datasets and analysis of positioning solutions by ingesting various sets of water vapor data into PPP are discussed in Section 3. In the final Section the conclusion and future work are summarized.

2 Data and method

In May 2014 one water vapor radiometer of model RPG-LWP-G4 manufactured by the Radiometer Physics,

Germany, and one GNSS receiver were installed on the campus of Tongji University (31.285°N, 121.498°E), Shanghai, China. The co-located WVR and GPS receiver is separated by about 1 m, and both can measure the pressure and temperature (Can GPS receiver measure pressure and temperature too???). GPS receiver is facilitated with TRIMBLE antenna and is referred as TJCH. Please give more details of the GPS Rx model and WVR model, manufacturers.

2.1 WVR

The RPG-LWP-G4 WVR operates at two K-band channel frequencies: 23.84 GHz and 31.4 GHz, with absolute brightness temperature accuracy of 0.5 K and the derived IWV has a nominal accuracy of 0.2 kg/m^2. The WVR can measure the IWV at both zenith and slant directions, and there are about 20,000 to 30,000 samples every day (be precise, how much time is needed for the WVR to complete one period of observation?) How is the observation performed? What is the azimuth interval? How is the elevation interval?). The IWV is retried (what is it?) using a neural network algorithm from measured brightness temperature. This algorithm is developed by the producer and set in the corresponding software. In this article WVR PWV data with rain flag is excluded, since the rain drop could cause large error (Shangguan et al., 2015) (Use Last name only) .

2.2 GPS data processing

(1) Reference coordinate

In order to get the "true" coordinate as a reference for the positioning accuracy analysis, the AUSPOS Online GPS Processing Service (http://www.ga.gov.au/bin/gps.pl) is utilized to compute the daily GPS positioning solution of GPS data collected from day of year (DOY) 156 to 365 in 2014 (Reza and Dare, 2006). AUSPOS selects about 13 stations (not about???? Be exact!) to form a local double-difference network. The baselines vary from 10 km to 2,000 km, with a mean length of about 500 km. The average ambiguity resolution success rate is 85%, which makes the AUSPOS solution reliable for this regional network. The standard Deviation) of AUSPOS solution in N/E/U direction is 3.1 mm, 6.0 mm and 8.0 mm, respectively. (This is very large!!!! Are these numbers calculated from 156 to 365 DOY daily solutions???) The coordinate's time series and daily bias are shown in Figure 1. In Figure 1a, the time series is plotted using the coordinates of DOY 150 as reference. It can be seen that the coordinates vary over time with a velocity. Considering the station's velocity, the coordinate is firstly linearly fitted to get the initial coordinate at epoch 2014.00 (DOY 001, 2014) and the corresponding velocity (what is the velocity in N, E, U????). In Figure 1b, the coordinate bias is calculated using the "true" position derived from the coordinate at epoch 2014.00 and corresponding velocity (not clear how to calculate the bias!!). Why not use BERNESE or GAMIT to calculate the reference solution by yourself?? You can use a nearby Chinese domestic station to calculate the Tongji station's coordinates. Using AUSPOS, it uses very long baselines since it uses Australian GPS stations as references.
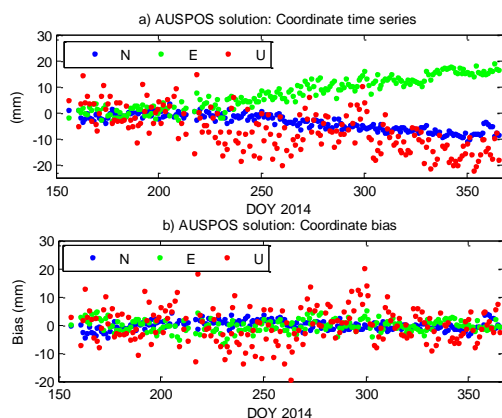

Figure 1 AUSPOS coordinate solution.

a) Coordinate time series; b) Coordinate bias

(2) GPS PWV derivation

Tropospheric delay in the signal transmitting path, i.e. slant tropospheric delay (STD), can be defined as following:

$$STD = mf_h \times ZHD + mf_w \times ZWD +$$
$$mf_w \times \cot E \times \left(G_N \cos\alpha + G_E \sin\alpha \right) \tag{1}$$

where ZHD and ZWD are the zenith hydrostatic the wet zenith delay, respectively; mf_h and mf_w are the hydrostatic and the wet mapping function, respectively; G_N and G_E are the delay gradient parameters in the north and eastern direction, respectively; E is the elevation angle, and α is the azimuth angle. ZWD is obtained by subtracting the ZHD from the estimated ZTD, while ZHD could be derived using the Saastamoinen model (Saastamoinen, 1972; Davis et al., 1985; Bevis et al., 1992),

$$ZHD = \frac{0.0022768 P_s}{1 - 0.0026 \cos(2\varphi) - 0.00028 h} \tag{2}$$

where P_s is atmospheric pressure at the height of GPS antenna (unit: hPa); φ is the geodetic latitude and h is the height above geoid (unit: km). Then the ZWD is converted into the PWV using surface temperature (Bevis et al., 1994),

$$PWV = \Pi \times ZWD \tag{3}$$

where Π is calculated following the approach of *Aske and Norduis* (1987) (Just give the value of II you used in this paper. It needs to be concise)

Accurate ZTD is estimated from GPS observations using the Bernese 5.0 software in PPP strategy (Dach et al., 2007). Saastamoinen model is used to calculate a priori zenith hydrostatic delay. The zenith wet delay as well as the gradients are estimated as constant each hour. A cutoff elevation of 10 degrees is adopted and the precise orbit and precise satellite clock data from the IGS (International GNSS Service) final products are used. The ZWD, GPS station static coordinates and other parameters are estimated (What are the other parameters???).

The Bernese PPP daily coordinate solution is shown in Figure 2, and the statistics are shown in Table 1. In both Figure 2 and Table 1, the bias is estimated from daily static PPP solution by using the AUSPOS solution as reference. The RMS of Bernese PPP solution for the period DOY 156 to 365, 2014 are 6.5 mm, 9.7 mm, and 9.5 mm in north, east and up directions, respectively. According to *Hill et al.* (2009), the ZTD accuracy is approximately one-third of the accuracy in the up direction. Thus, the PWV accuracy from Bernese PPP solution is estimated to be about 0.5 mm.
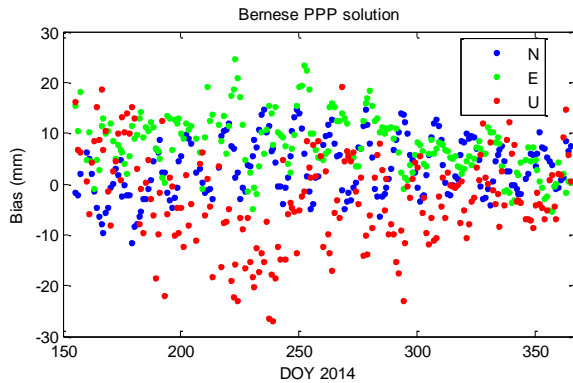
Figure 2 Bernese PPP solution: Coordinate bias

Table 1 Statistics of Bernese PPP solution (mm)

	N	E	U
Mean	3.3	7.8	-3.0
SD	5.6	5.7	9.1
RMS	6.5	9.7	9.5

The PWV data series should be plotted in this section.

(3) WVR assisted PPP

The purpose of this study is to evaluate how the WVR water vapor data can contribute to improve the PPP accuracy. In order to perform this evaluation four PPP strategies are used as shown in Table 2. In the WVR mode, the ZHD is calculated using in situ meteorological data, and ZWD is derived from WVR data using equation (3). In MET and GPT2 modes, ZHD and ZWD are fixed using in situ meteorological data, GPT2 model (it is hard to understand) (Lagler et al., 2013). In the EST strategy, the ZWD is estimated every one hour. In all these four modes the VMF1_ht (Boehm et al., 2006a) mapping function is used to map the zenith delay to satellite's signal transmitting path. PPP is carried using self-developed software, referred as NetPPP in this paper.

Table 2 Description of different PPP strategies

	ZHD	ZWD
WVR	Met data	WVR, fixed
EST	GPT2	Estimated
GPT2	GPT2	GPT2, fixed
MET	Met data	Met data*, fixed

Note: "Met data" is short for meteorological data

The four types of PPP are carried in both static and kinematic modes. Besides, the static PPP mode has several cut-off elevation settings in order to investigate the influence of WVR assisted PPP in different circumstance, including 5°, 7°, 10°, 15°, 20°, 25°, and 30°. The cut-off elevation of kinematic PPP is 10°. It should be noted that the WVR data is only from DOY 156 to 305, 2014, due to the data deficiency. Therefore, in this part the PPP is performed using GPS data from DOY 156 to 305, 2014, and all the following PPP analyses are based on this time period.

3 Analysis and result

3.1 PWV comparison

The PWV derived from Bernese PPP solution is firstly compared with PWV from WVR, ECMWF and radiosonde. The ERA Interim surface PWV (Balsamo et al., 2012) data with a sample of 0.125°×0.125° in latitude and longitude are used. ERA Interim surface data provide surface temperature, pressure, PWV four times a day at UT 00, 06, 12 and 18. A bio-linear (do you mean bio-linear or bi-linear????) interpolation is utilized to get the PWV for the TJCH station. In addition, a radiosonde station (WMO ID: 58362), which is located about 16 km away from TJCH station, is also selected for PWV comparison.

The time series of GPS PWV and WVR PWV, as well as the PWV bias are shown in Figure 3 and Figure 4, respectively. In Table 3, the statistics of PWV differences between GPS, WVR, ECMWF and radiosonde are summarized. A linear fitting between GPS PWV and WVR PWV, as shown in Figure 4a and the fitting residual is shown in Figure 4c.

with 23 out of 2466 biases (~0.9%) are larger than three times of standard deviation, which are regarded as gross

It should be noted that in Figure 3, Table 3 and subplot b), Figure 4 the PWV bias between GPS and WVR are calculated before the line fitting (. I think it is more appropriate to remove the gross error data point before you calculate).
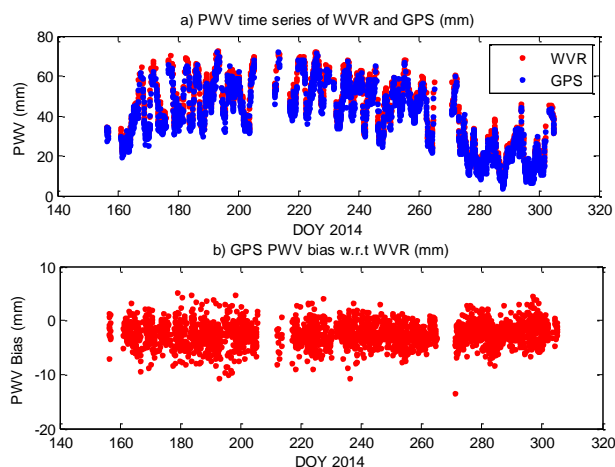

Figure 3 PWV time series and bias

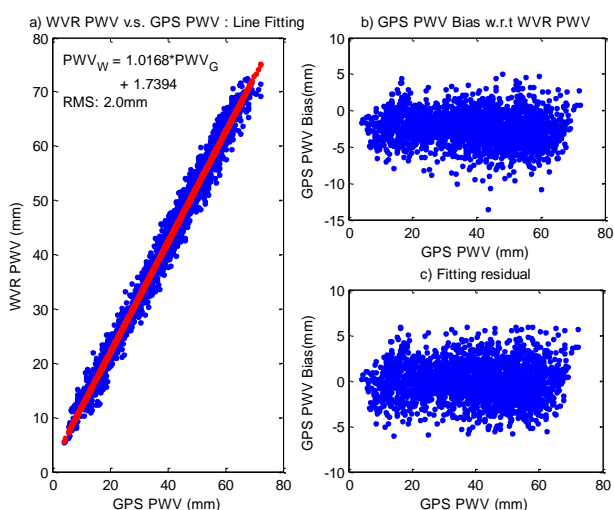a) PWV time series from GPS and WVR; b) GPS PWV bias w.r.t. WVR PWV

Figure 4 GPS PWV and WVR PWV fitting result

a) Line fitting; b) Raw PWV bias; c) PWV fitting residual

Table 3 Statistics of PWV difference (mm)

	MEAN	SD	RMS	MAX	MIN
GPS－WVR	-2.4	2.1	3.2	5.1	-13.5
ECWMF－WVR	-0.9	2.6	2.7	12.9	-13.5
RS－WVR	-0.9	3.5	3.6	12.3	-15.4
ECMWF－GPS	1.6	3.1	3.4	12.9	-7.6
RS－GPS	1.4	3.6	3.9	11.0	-8.1

Note: The number of each comparison is 2466, 681, 212, 611, and 189, respectively.

From Table 3 we can see that the standard deviation of the differences between GPW PWV and WVR PWV is smaller than others, while the mean bias (MEAN) is much larger than that of other comparisons. The RMS between radiosonde PWV and WVR PWV, as well as radiosonde PWV and GPS PWV are larger than others. This may be

because of the large distance (16 km) between the radiosonde station and the co-located WVR/GPS station as well as large water vapor gradient in a humid environment like Shanghai.

Noticing the mean discrepancy between GPS PWV and WVR PWV is as large as 2.4 mm, which is larger than the one reported by other researchers. Therefore, we firstly compare the different Tm ~ Ts (what is Tm ?? What is Ts???) relationships between Bevis equation (reference paper for Bevis equation????) and others. *Yao et al.* (2014) gave a sophisticated Tm ~ Ts relationship based on ECMWF data. However, the difference between Yao and Bevis at TJCH station is less than 3 K therefore the corresponding PWV difference caused by Tm ~ Ts equation error should be about 1% (how do you get the 1%??? Why not 2% or others?). Taken the mean value of PWV in TJCH, which is about 40 mm, then the PWV bias caused by Tm ~ Ts relationship is about 0.4 mm, which is much smaller than 2.4 mm. (similarly why 1%??) Secondly, the PWV uncertainty from GPS should be less than 0.5 mm, considering the coordinate accuracy in Table 1. Therefore, this large discrepancy is not purely caused by the Tm calculation error or PPP error.

We take a careful look at the GPS-WVR PWV bias and its relationship with meteorological observations, including in situ pressure, temperature, relative humidity, liquid water path (LWP), as well as PWV. The GPS-WVR PWV bias with respect to atmosphere observations is shown in Figure 4b and Figure 5. No explicit relationship between PWV bias and meteorological observations is revealed. The bias between GPS-WVR PWV does not vary much while the PWV or other meteorological observations vary. In addition, if we take the WVR observations as true value, the GPS PWV bias caused by ZTD error should be as large as 1.6 mm (80% of 2.4 mm) according to *Ning et al.* (2016). Such a large bias is equivalent to 1 cm bias ZTD. Hence, the corresponding coordinate bias in up direction is about 3 cm, which is much larger than PPP accuracy.

Therefore, we consider this large discrepancy as systematic error, which may be caused by the following reasons: (1) the calibration of WVR could only assure the accuracy of measured brightness temperature, but not the algorithm to derive PWV from brightness temperature; (2) the algorithm to derive PWV from measured brightness temperature uses radiosonde PWV data as reference, while the difference between radiosonde PWV and GPS PWV could be large; (4) the error introduced by Saastamoinen model to calculate ZHD could be as large as 8 mm in China (Chen and Liu, 2015). The ZHD is normally held as true value thus the error in the ZHD can propagate into the determination of GPS PWV. (I am a little confused by what you are trying to express. Do you want to talk about the WVR PWV error source, or radiosonde PWV error source, or the GPS PWV error source???)
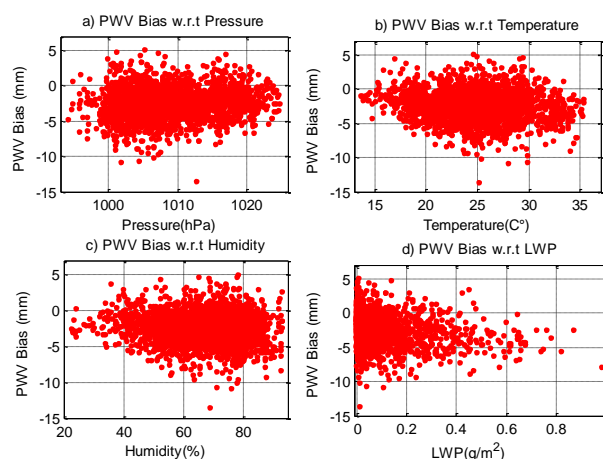

Figure 5 PWV Bias between GPS and WVR (The caption of all the figures, tables should be as detailed as possible. They are too short and contain almost no information)

3.2 PPP result

As shown above, a large discrepancy (mean bias: 2.4 mm, RMS: 3.2 mm) between GPS-WVR PWV differences.

To remove the systematic error in the WVR PWV data, the observed WVR PWV is calibrated using the following equation:

$$PWV_{W1} = 0.9836 \times PWV_W - 1.7101 \qquad (4)$$

where PWV_{W1} (I suggest the PWV_wc be used, not PWV_w1) is the calibrated WVR PWV and PWV_W is the raw WVR observation. After the calibration, the RMS between calibrated WVR PWV and GPS PWV is 2 mm, which is also shown in Figure 4a.

First the static PPP of all the four strategies, which are described in Table 2, were conducted with different cut-off elevation sets. The RMS and MAE (Mean Absolute Error) of each daily solution are calculated as following:

$$RMS = \frac{1}{n}\sum_{i=1}^{n}(\Delta_i)^2$$
$$MAE = \frac{1}{n}\sum_{i=1}^{n}DMAE_i \qquad (5)$$
$$DMAE = \frac{1}{m}\sum_{j=1}^{m}\left|\Delta_j^{epoch}\right|$$

where Δ_i is the bias of each daily solution with respect to reference solution (I think your RMS should have ROOT SQUARE!!!!); $DMAE_i$ is the daily mean absolute error (DMAE); and Δ_j^{epoch} is the bias of epoch j PPP solution with respect to the reference solution; n is the number of days and m is the number of epochs. The first 3 hour PPP solutions are not used in the statistics due to convergence issue.

Table 4 RMS of each strategy with different cut-off elevations (cm)

Cut-off elevation	EST			WVR			GPT2			MET		
	N	E	U	N	E	U	N	E	U	N	E	U
5°	0.89	0.50	1.81	0.87	0.53	1.62	0.96	1.37	21.49	1.01	1.46	24.47
7°	0.89	0.50	1.79	0.87	0.53	1.62	0.96	1.36	21.47	1.01	1.45	24.46
10°	0.86	0.53	1.65	0.87	0.53	1.63	0.91	1.09	19.57	0.94	1.13	21.96
15°	0.83	0.52	1.39	0.82	0.54	1.70	0.87	1.03	18.59	0.89	1.00	20.80
20°	0.78	0.54	1.64	0.77	0.58	1.65	0.79	1.03	16.67	0.82	0.96	18.58
25°	0.73	0.61	4.12	0.71	0.66	1.55	0.73	1.06	14.75	0.75	1.00	16.43
30°	0.72	0.69	7.63	0.69	0.74	1.31	0.71	1.07	13.05	0.73	1.02	14.58

Table 5 MAE of each strategy with different cut-off elevations

Cut-off elevation	EST			WVR			GPT2			MET		
	N	E	U	N	E	U	N	E	U	N	E	U
5°	0.93	0.93	2.01	0.88	0.93	1.75	1.18	2.20	20.25	1.21	2.48	22.18
7°	0.93	0.93	1.99	0.88	0.94	1.75	1.18	2.18	20.23	1.21	2.46	22.15
10°	0.90	0.91	1.89	0.87	0.95	1.76	1.09	1.82	18.24	1.11	2.00	19.38
15°	0.87	0.90	1.85	0.87	0.94	1.77	0.99	1.61	17.24	1.03	1.69	18.29
20°	0.85	0.94	2.54	0.84	0.96	1.77	0.88	1.35	15.36	0.90	1.40	16.25
25°	0.81	0.99	4.79	0.79	1.04	1.74	0.82	1.22	13.54	0.83	1.24	14.29
30°	0.83	1.09	7.56	0.79	1.14	1.69	0.80	1.23	11.92	0.83	1.25	12.61

Table 6 Daily repeatability of each strategy with different cut-off elevations (cm)

Cut-off elevation	EST			WVR		
	N	E	U	N	E	U
5°	0.43	0.51	1.30	0.43	0.49	1.12
7°	0.43	0.51	1.30	0.43	0.49	1.12
10°	0.41	0.53	1.23	0.42	0.49	1.12
15°	0.37	0.52	1.33	0.38	0.52	1.12
20°	0.33	0.54	1.58	0.34	0.56	1.04
25°	0.31	0.59	3.06	0.30	0.64	1.03
30°	0.29	0.67	5.95	0.29	0.72	1.03

Table 4 and Table 5 show that for both EST and WVR strategies, the RMS of PPP positioning errors in horizontal and up directions are smaller than 1 cm and below 2 cm, respectively, for cut-off elevation below 20°. For cut-off elevation below 20°, The WVR mode performs a little better (about 1~2 mm) than the EST mode in the up direction, which shows the advantage of using WVR data as fixed values in ZTD correction. For high cut-off elevation circumstances (above 20° in this paper), the accuracy in up direction for the EST mode decreases significantly (~7 cm) with the increase of cut-off elevation. This is likely caused by the poor observation geometry and reduced observation data in the high cut-off elevation circumstance. Therefore, it is expected that if the ZTD is fixed accurately, the accuracy should not show large fluctuation, especially in up direction. This is confirmed by the results of WVR mode shown in both Table 4 and Table 5, where the WVR data are held fixed to correct ZTD in the PPP computation. We can see that the accuracy in high cut-off elevations remains the same as low cut-off elevations. Furthermore, the RMS in up direction is 1.31 cm when the cut-off elevation is 30°, which is 3.4 mm smaller than the RMS of 1.65 cm at 20°. We consider this as the benefit resulting from the reduction of mapping function error in high cut-off elevation. We also calculate the daily coordinate repeatability which indicates the PPP solution internal consistency (Kouba, 2009) of EST and WVR strategies, as shown in Table 6. Table 6 also shows that the WVR mode results in a better accuracy than the EST mode under different cut-off elevation circumstances, confirming that fixing the calibrated WVR PWV data using Eq. (7) can enhance the PPP accuracy.

Another benefit of fixing WVR PWV data in PPP is the acceleration of ambiguity convergence. Table 7 shows statistics of the time to converge to 10 cm in all directions (N/E/U). In the EST mode the mean convergence time is about 1.1 ~ 2 hours at cut-off elevations below 20°, which is much longer than that of WVR mode (~0.8 hour). For cut-off elevations above 20°, the convergence time is much longer than that of low cut-off elevations. However for the WVR mode, the convergence time remains shorter than 1 hour.

Table 7 Statistics of convergence time in different cut-off elevation

Cut-off elevation	MEAN (h)		MEDIAN (h)	
	EST	WVR	EST	WVR
5°	1.15	0.75	1.04	0.54
7°	1.15	0.74	1.02	0.54
10°	1.14	0.74	0.95	0.54
15°	1.48	0.77	1.33	0.58
20°	2.05	0.80	1.70	0.63
25°	3.81	0.84	2.68	0.72
30°	8.98	0.96	3.80	0.85

In addition, Table 4 and Table 5 show that if the ZTD is fixed using GPT2 data or meteorological observation,

the accuracy in up direction is much worse than that of EST and WVR strategies. This degradation clearly is due to inaccurate fixing of ZTD. The ZTD calculated from the GPT2 and meteorological data have been compared with ZTD from Bernese PPP estimation and the RMS values are 7.0 cm and 6.5 cm, respectively. Therefore, the corresponding RMS in up direction should be about three times of ZTD, which is about 20 cm. This is confirmed in Table 4 and Table 5. However, in high cut-off elevation circumstances (>20°) the RMS reduces to about 13 cm in up direction. This is due to the discard of low elevation observations, which has a larger tropospheric delay due to the fixing of an inaccurate ZTD than that of observations in high elevations.

Table 8 Statistics of kinematic PPP accuracy (cm)

	RMS			MAE		
	N	E	U	N	E	U
EST	4.43	5.14	11.55	3.11	3.57	8.44
WVR	5.41	6.41	11.28	3.26	3.78	7.25
GPT2	6.42	8.02	23.91	4.94	5.62	19.45
MET	6.82	8.13	25.26	5.11	5.81	20.54

We also conducted a kinematic PPP campaign and the statistics of daily RMS and MAE are shown in Table 8. With an RMS of 7.25 cm in the up direction, the WVR mode also performs a better accuracy than the EST mode (8.44 cm in the up direction). For the GPT2 and MET modes, the horizontal accuracy is about 5 ~ 8 cm while the up accuracy is about 20 cm. Apparently, both EST and WVR mode have much better performance than the GPT and MET modes.

4 Conclusions

The PWV observation data collected from GPS, WVR, ECMWF and radiosonde are compared and analyzed in this paper. A large discrepance between the GPS PWV and WVR PWV exists, which results in a bias up to 2.4 mm and RMS up to 3.2 mm. The PWV differences between GPS, ECMWF and radiosonde are also large.

Both static and kinematic GPS PPP experiments are conducted to investigate the accuracy improvement by through PPP augmentation by fixing calibrated WVR PWV to correct ZWD error. As a comparison, tests have been conducted by fixing the ZWD derived from meteorological data and GPT2 model. The performance of three sets of ZWD-fixing PPP solutions is compared with that of regular PPP where the ZWD is estimated as a parameter. The static PPP tests have been performed under different cut-off elevations. It shows that when ZWD is fixed using calibrated WVR PWV the accuracy improves a little (how many percentages!!!) compared with that of regular ZWD estimation strategy in both static and kinematic modes. At high cut-off elevations (>20°), the static PPP accuracy degrades significantly to 7 cm (be exact: 7.xxxx cm) when ZWD is estimated at the cut-off elevation 30°, while in WVR-augmented static PPP the accuracy yields the same (how many cm exactly???). Moreover, the convergence time is much shorter in WVR assisted PPP (how shorter??? Be exact!).

Reference

Askne, J., and H. Nordius (1987), Estimation of tropospheric delay for microwaves from surface weather data, Radio Sci., 22, 379–386, doi:10.1029/RS022i003p00379.

Beckman, B, 1985. A Water-Vapor Radiometer Error Model, in Geoscience and Remote Sensing, IEEE Transactions on , 23(4), pp.474-478. doi: 10.1109/TGRS.1985.289437

Bevis, M., Businger, S., Herring, T. A., Rocken, C., Anthes, R. A., and Ware, R. H. GPS meteorology: Remote sensing of atmospheric water vapor using the Global Positioning System, J. Geophys. Res., 97, 15787–15801, doi:10.1029/92JD01517, 1992.

Bevis, M., Businger, S., Chiswell, S., Herring, T. A., Anthes, R. A., Rocken, C., and Ware, R. H. GPS meteorology: Mapping zenith wet delays onto precipitable water, J. Appl. Meteorol., 33, 379–386, 10.1175/1520-0450(1994)033<0379:GMMZWD>2.0.CO;2, 1994.

Biyan Chen, ZhiZhao Liu. 2015. A comprehensive evaluation and analysis of the performance of multiple tropospheric models in China Region. IEEE.

Boehm, J., Werl, B., and Schuh, H. Troposphere mapping functions for GPS and very long baseline interferometry from European Centre for Medium-Range Weather Forecasts operational analysis data, J. Geophys. Res.-Sol. Ea., 111, B02406, doi:10.1029/2005JB003629, 2006a.

Boehm, J., Niell, A., Tregoning, P., and Schuh, H. Global Mapping Function (GMF): A new empirical mapping function based on numerical weather model data, Geophys. Res. Lett., 33, L07304, doi:10.1029/2005GL025546, 2006b.

Christian Rocken, James Johnson, Teresa Van Hove, et al. 2005. Atmospheric water vapor and geoid measurements in the open ocean with GPS. Geophysical Research Letters, Vol.32, L12813. doi:10.1029/2005GL022573

Cuixian Lu, Xingxing Li, Zhenghong Li, et al. 2016. GNSS tropospheric gradients with high temporal resolution and their effect on precise positioning. Journal of Geophysical Research atmospheres. 2016. doi: 10.1002/2015JD024255

Dach R, Hugentobler U, Fridez P, Meindl M (eds) (2007) Bernese GPS software version 5.0, 612, Astronomical Institute, University of Bern

Davis, J. L., T. A. Herring, I. I. Shapiro, A. E. E. Rogers, and G. Elgered (1985), Geodesy by radio interferometry: Effects of atmospheric modeling errors on estimates of baseline length, Radio Sci., 20, 1593–1607.

Duan, J., and Coauthors, 1996. GPS meteorology: Direct estimation of the absolute value of precipitable water. J. Appl. Meteor., 35, 830–838.

Emardson, T. R., G. Elgered, and J. M. Johansson (1998), Three months of continuous monitoring of atmospheric water vapor with a network of GPS receivers, J. Geophys. Res., 103, 1807– 1820.

Fang, P., M. Bevis, Y. Bock, S. Gutman, and D. Wolfe (1998), GPS meteorology: Reducing systematic errors in geodetic estimates for zenith delay, Geophys. Res. Lett., 25, 3583-3586.

G. Balsamo, C. Albergel, A.C.M. Beljaars, et al. 2012. ERA-Interim/Land: A global land-surface reanalysis based on ERA-Interim meteorological forcing, ERA Report Series, ECMWF.

Gendt, G., G. Dick, C. Reigber, M. Tomassini, Y. Liu, and M. Ramatschi (2004), Near real time GPS water vapor monitoring for numerical weather prediction in Germany, J. Meteorol. Soc. Jpn., 82, 361-370.

Gunnar Elgered et al. 2012. Assessing the Quality of Water Vapor Radiometer Data from Onsala during the CONT11 Geodetic VLBI Campaign, IVS 2012 General Meeting Proceedings, p.410-414

Hill, E. M., J. L. Davis, P. Elo´segui, B. P. Wernicke, E. Malikowski, and N. A. Niemi (2009), Characterization of sitespecific GPS errors using a short-baseline network of braced monuments at Yucca Mountain, southern Nevada, J. Geophys. Res., 114, B11402, doi:10.1029/2008JB006027.

John Braun, Christian Rocken, and James Liljegren, 2003: Comparisons of Line-of-Sight Water Vapor Observations Using the Global Positioning System and a Pointing Microwave Radiometer. J. Atmos. Oceanic Technol., 20, 606–612. doi: http://dx.doi.org/10.1175/1520-0426(2003)20<606:COLOSW>2.0.CO;2

J. Kouba. Implementation and testing of the gridded Vienna Mapping Function 1 (VMF1). J Geod (2008) 82:193– 205. DOI 10.1007/s00190-007-0170-0

Lagler, K., M. Schindelegger, J. Böhm, H. Krásná, and T. Nilsson (2013), GPT2: Empirical slant delay model for radio space geodetic techniques, Geophys. Res. Lett., 40, 1069–1073, doi:10.1002/grl.50288.

Li, X., F. Zus, C. Lu, G. Dick, T. Ning, M. Ge, J. Wickert, and H. Schuh (2015a), Retrieving of atmospheric parameters from multi-GNSS in real time: Validation with water vapor radiometer and numerical weather model.

J. Geophys. Res. Atmos., 120, 7189–7204. doi:10.1002/2015JD023454.

Michal KAČMAŘÍK, Jan DOUŠA, Jan ZAPLETAL. 2012. Comparison of GPS slant wet delays acquired by different techniques. Acta Geodyn. Geomater., Vol. 9, No. 4 (168), 427–433, 2012

Miloshevich, L.M., H. Vömel, D.N. Whiteman, and T. Leblanc (2009), Accuracy assessment and correction of Vaisala RS92 radiosonde water vapor measurements. J. Geophys. Res., 114, D11305, doi:10.1029/2008JD011565.

Miloshevich, L.M., H. Vömel, D.N. Whiteman, B.M. Lesht, F.J. Schmidlin, and F. Russo (2006), Absolute accuracy of water vapor measurements from six operational radiosonde types launched during AWEX-G and implications for AIRS validation. J. Geophys. Res., 111, doi:10.1029/2005JD006083

M. Shangguan, S. Heise1, M. Bender, G. Dick, M. Ramatschi, and J. Wickert. Validation of GPS atmospheric water vapor with WVR data in satellite tracking mode. Ann. Geophys., 33, 55–61, 2015. doi:10.5194/angeo-33-55-2015

Reza Ghoddousi-Fard, Peter Dare. 2006. Online GPS processing services: an initial study. GPS Solution (2006) 10:12-20. DOI: 10.1007/s10291-005-0147-5

Randolph Ware, Christian Rocken, Fredrick Solheim, et al. 1993. Pointed water vapor padiometer corrections for accurate global positioning system surveying. Geophysical Research Letters, Vol. 20, No.23, pp. 2635-2638

Rocken, C., T. Van Hove, and R. Ware (1997), Near real-time sensing of atmospheric water vapor, Geophys. Res. Lett., 24, 3221-3224.

Tregoning, P., R. Boers, D. O'Brien, and M. Hendy, 1998: Accuracy of absolute precipitable water vapor estimates from GPS observations. J. Geophys. Res., 103, 28 701–28 710.

T. Ning, J. Wang, G. Elgered, G. Dick, J. Wickert, M. Bradke, M. Sommer, R. Querel, and D. Smale. The uncertainty of the atmospheric integrated water vapour estimated from GNSS observations. Atmos. Meas. Tech., 9, 79-92, 2016. doi:10.5194/amt-9-79-2016

Wang, J., L. Zhang, and A. Dai, 2005. Global estimates of water-vapor-weighted mean temperature of the atmosphere for GPS applications. J. Geophys. Res., 110, D21101, doi:10.1029/2005JD006215.

Wang, J., L. Zhang, A. Dai, T. Van Hove, J. Van Baelen, 2007: A near-global, 2-hourly data set of atmospheric precipitable water from ground-based GPS measurements. Journal of Geophysical Research, 112, D11107. 10.1029/2006JD007529.

Yao Y B, Zhang B, Xu C Q, et al. Analysis of the global Tm-Ts correlation and establishment of the latitude-related linear model. Chin Sci Bull, 2014, 59, doi: 10.1007/s11434-014-0275-9

Yuei-An Liou, Yu-Tun Teng, Teresa Van Hove, and James C. Liljegren, 2001: Comparison of Precipitable Water Observations in the Near Tropics by GPS, Microwave Radiometer, and Radiosondes. J. Appl. Meteor., 40, 5–15. doi: http://dx.doi.org/10.1175/1520-0450(2001)040<0005:COPWOI>2.0.CO;2

Zhizhao Liua, Min Lia, Weikun Zhonga, Man Sing Wonga. An approach to evaluate the absolute accuracy of WVR water vapor measurements inferred from multiple water vapor techniques. Journal of Geodynamics, vol.72, 86-94, 2013. doi:10.1016/j.jog.2013.09.002

Saastamoinen, J. 1972. "Atmospheric Correction for the Troposphere and Stratosphere in Radio Ranging Satellites." In *The Use of Artificial Satellites for Geodesy*, 15:247–51. Geophys. Monogr. Ser. Washington, DC: AGU. http://dx.doi.org/10.1029/GM015p0247.